JOURNAL OF THERMOPHYSICS AND HEAT TRANSFER
Vol. 12, No. 1, January–March 1998

Radiative Properties of Fiber-Reinforced Aerogel: Theory Versus Experiment

G. R. Cunnington* and S. C. Lee†
Applied Sciences Laboratory, Inc., Hacienda Heights, California 91745
and
S. M. White‡
NASA Ames Research Center, Moffett Field, California 94035

This paper presents a theory and its validation by experiment for the radiative properties of high-porosity silica aerogels that contain randomly oriented and uniformly dispersed fibers. The formulations for the fiber radiative properties are based on fundamental principles, for which parameters defining the material composition are the only required inputs. The predicted spectral transmittance and reflectance for collimated irradiation from the solution of the radiative transfer equation are compared with the measured values. The validity of the theoretical model is established by the good agreement between the predictions and experimental data for various specimens that contain different fiber types, fiber and aerogel solid volume fractions, and specimen thicknesses.

Nomenclature

d^2F = fiber orientation distribution function
f_v = fiber volume fraction
I_λ = spectral intensity
$i(\eta, \phi)$ = isolated fiber scattering intensity distribution
K_λ = spectral extinction coefficient
L = specimen thickness
N = number of fiber sizes
p_λ = spectral phase function
Q = single fiber efficiency
R_h = hemispherical reflectance
r = fiber radius
T_n = normal transmittance
x_i = fractional volume of fibers of radius r_i
η = scattering angle
μ = direction cosine of angle ξ
ξ = polar angle of incidence direction
σ_s = scattering coefficient
ϕ = incidence angle
ω = azimuthal angle of incidence direction

Subscripts

e = extinction
f = fiber
m = fiber and aerogel mixture
s = scattering
λ = wavelength
0 = aerogel matrix

Introduction

FIBROUS materials are widely used for thermal insulation at ambient and high temperatures in many commercial and aerospace applications. Fibrous thermal insulations generally consist of either self-supporting bonded fibers, loosely packed fibers, or unbonded fibers dispersed in a matrix medium. The first type is typical of the Space Shuttle thermal protection tile materials, the second type is usually found in building insulations, and the last type corresponds to structural composites that contain a relatively high density of fibers. The high-density fibrous composites are generally not suitable for applications in which weight is a critical issue. A novel lightweight fibrous insulation is the fiber-loaded aerogel that can be applied at moderate to high temperatures.

Aerogel is an open-cell, partially infrared transparent super-insulator first developed over 60 years ago by Kistler.[1] It has unique properties resulting from the chemical preparation method that produces an extremely low-density solid having a skeletal structure with pores of the order of 10 nm in diameter. The low density and very small pores combine to give the aerogel low thermal conductivity at or near atmospheric pressure. The fine microstructure impedes gas conduction because at modest vacuum pressures, the collision rate of gas molecules is dominated by the collision rate with the lattice-like structure of the aerogel, thus resulting in the Knudsen number being unity or larger. Solid thermal conductivities as low as 0.02 W/m-K and 0.007 W/m-K have been reported for air-filled and partially evacuated (0.1 atm) silica aerogel, respectively.[2] At ambient and higher temperatures, radiative absorption/emission become the dominant heat transfer mechanism. Aerogel is a poor thermal insulation because it is highly transparent in the 3–8 μm wavelength region. Models for heat transfer through monolithic aerogel generally treat the conduction and radiation as additive contributions by defining an effective radiative conductivity.[3–5] To improve its thermal insulation capacity, approaches such as doping aerogel with carbon have been applied to minimize infrared radiation heat transfer.[3] By incorporating fibers into the aerogel matrix, the fibers suppress radiation transport by eliminating the infrared transparent window of aerogel and also strengthen the otherwise extremely brittle monolithic aerogel. An appropriate selection of fiber type and concentration is critical to optimizing the thermal insulation capacity of the material, especially at high temperatures. A fundamental understanding of the radiative properties of fibrous aerogel is therefore essential to improving the thermal insulation effectiveness of this type of material.

The objective of the present study is to develop and validate a rigorous theoretical model that does not require the use of empirical parameters. This contrasts with the commonly applied inversion analyses that are usually applied in the absence

Received Dec. 30, 1996; revision received May 16, 1997; accepted for publication May 16, 1997.

*Consultant. Associate Fellow AIAA.
†Vice President. Senior Member AIAA.
‡Research Scientist. Member AIAA.

of a rigorous theoretical model for the radiative properties. The inversion approach involves the determination of the radiative properties by curve fitting the experimental data. An obvious deficiency of inversion is that the empirically determined parameters usually do not have any correspondence with the physical material parameters. Furthermore, inversion cannot be used to tailor the material composition to achieve the desired thermal performance. Nevertheless, it offers a means of determining properties for immediate use in heat transfer calculations for the material.

This paper presents a theoretical model and its experimental validation for the radiative properties of fiber-loaded aerogels. The theory consists of modeling the extinction and scattering coefficients and phase function of the fiber-loaded aerogels from fundamental principles. Only deterministic physical characteristics of the material are required as inputs for calculating the radiative properties. The theoretical radiative properties are then used in the radiative transfer equation to compute the spectral transmission and reflection. The experimental study includes measurements of spectral transmission and reflection of various fibrous aerogel specimens. The theoretical predictions are compared with test data to determine the adequacy of the theoretical model. The current theoretical model extends beyond that presented in a previous article,[6] which considered self-supporting fibrous media containing bonded fibers in air/vacuum. In the present paper, we consider composites of unbonded fibers dispersed in a spectrally dependent absorbing matrix. Validation of the present model would then provide the general capability, in conjunction with the model presented in Ref. 6, to treat high-porosity fibrous materials with and without an intervening matrix medium. In the following sections, the theoretical model is first described, then followed by discussions of the experiment and model validation.

Theory

The fibrous aerogels under consideration have nominal bulk densities between 100–160 kg/m^3, which correspond to less than 6% total solid volume fraction, and the fiber volume fraction ranges from 0.01 to 0.02. Because of the high porosity, the fibers can be assumed to scatter independently. The fibers are several millimeters long and about 3 μm in diameter. They are modeled as infinite cylinders because their length is much greater than both the diameter and the wavelength of thermal radiation. Examination of the specimens indicate that the fibers are randomly oriented in the aerogel matrix.

The theory of light scattering by an isolated infinite cylinder is well established in the literature. A summary of the formulation for scattering by an infinite cylinder at oblique incidence is given in Kerker.[7] Infinite cylinders behave as two-dimensional scatterers for which the scattered radiation propagates along the surface of a cone with an apex angle equal to $\pi - 2\phi$, where the angle of incidence ϕ is measured from the normal to the fiber axis. The extinction and scattering cross sections of a fiber then vary with the angle of incidence. Consequently, the radiative properties of a dispersed medium of fibers also vary with the orientation of the fibers. The theoretical models that account for fiber orientation have been presented by Lee.[8–10]

To compute the radiative properties of high-porosity fibrous media, both orientation and size distribution of fibers are considered. Using Lee's theoretical models,[8–10] the extinction and scattering coefficients accounting for these effects are summarized as

$$(\kappa_\lambda,\ \sigma_{s\lambda}) = \int_{\omega_{f1}}^{\omega_{f2}} \int_{\xi_{f1}}^{\xi_{f2}} \int_{r_1}^{r_2} 2r(Q_{e\lambda},\ Q_{s\lambda}) N(r)\ \mathrm{d}r d^2F(\xi,\ \omega) \quad (1)$$

where $Q_{e\lambda}$ and $Q_{s\lambda}$ are the theoretical spectral extinction and scattering efficiencies, respectively. Expressions for these efficiencies are well summarized in many texts, such as in Kerker.[7] The difference between the extinction and scattering coefficients gives the absorption coefficient. In Eq. (1) (ξ_{f1}, ξ_{f2}) and (ω_{f1}, ω_{f2}) denote the range of the polar and azimuthal orientations of the fibers for the orientation distribution function d^2F. In general, these radiative coefficients vary with the incident direction, except for the special case of fibers randomly oriented in space. Because the scattering cross section of a fiber varies with the incidence angle, the product of the scattering coefficient and phase function (p_λ) must be considered as a group. For a given incident direction specified by (ξ, ω), this product is given by

$$\langle \sigma_{s\lambda} p_\lambda(\eta) \rangle = \frac{4\lambda}{\pi^2} \int_{\omega_{f1}}^{\omega_{f2}} \int_{\xi_{f1}}^{\xi_{f2}} \int_{r_1}^{r_2} \times \frac{i(\eta,\ \phi)}{\sqrt{(1 - \cos\eta)(1 + \cos\eta - 2\sin^2\phi)}} N(r)\ \mathrm{d}r d^2F(\xi,\ \omega) \quad (2)$$

The scattering angle η is related to the incident (ξ, ω) and scattered (ξ', ω') directions by

$$\cos\eta = \mu\mu' + [(1 - \mu^2)(1 - \mu'^2)]^{1/2} \cos(\omega - \omega') \quad (3)$$

where $\mu = \cos\xi$. These equations for fibrous media are applied to model the fiber-loaded aerogels.

The fiber-loaded aerogels contain discrete size distributions of fibers randomly oriented in the aerogel matrix. Because aerogel is a purely absorbing material, the extinction coefficient of fiber-loaded aerogels can be modeled as a sum of that caused by fibers and aerogel:

$$K_{m\lambda} = K_\lambda + K_{0\lambda} \quad (4)$$

where $K_{0\lambda}$ is the absorption coefficient of the aerogel. The fiber extinction and scattering coefficients follow from Eq. (1) as

$$(K_\lambda,\ \sigma_{s\lambda}) = \frac{2f_v}{\pi} \sum_{i=1}^{N} \frac{x_i}{r_i} \int_0^{\pi/2} [Q_{e\lambda}(\phi),\ Q_{s\lambda}(\phi)] \cos\phi\ \mathrm{d}\phi \quad (5)$$

The scattering coefficient-phase function product is given by

$$\sigma_{s\lambda} p_\lambda(\eta) \rangle = \frac{4f_v\lambda}{\pi^4} \sum_{i=1}^{N} \frac{x_i}{r_i^2} \int_0^{\pi/2} \times \frac{i(\eta,\ \phi)}{\sqrt{(1 - \cos\eta)(1 + \cos\eta - 2\sin^2\phi)}} \cos\phi\ \mathrm{d}\phi \quad (6)$$

from which we obtain

$$\langle \sigma_{s\lambda} p_\lambda(\mu,\ \mu') \rangle = \frac{1}{2\pi} \int_0^{2\pi} \langle \sigma_{s\lambda} p_\lambda(\eta) \rangle\ \mathrm{d}\omega \quad (7)$$

for azimuthally independent boundary conditions.

The experimental data used to validate the theoretical model are spectral hemispherical reflectance and spectral normal transmittance of planar slabs of material illuminated with collimated irradiation at normal incidence. Given the theoretical radiative properties based on Eqs. (4–7), these quantities are predicted by solving the radiative transfer equation (RTE):

$$\mu \frac{\mathrm{d}I_\lambda}{\mathrm{d}y} + K_{m\lambda} I_\lambda = \frac{1}{2} \int_{-1}^{1} \langle \sigma_{s\lambda} p_\lambda(\mu,\ \mu') \rangle I_\lambda(\mu')\ \mathrm{d}\mu \quad (8)$$

for collimated incidence. Emission is neglected because the material is at room temperature. The boundary condition for incident intensity I_o is

$$I_\lambda(y = 0) = I_o\delta(\mu - 1) \tag{9}$$

where δ is the delta function.

The RTE is solved by the method of discrete ordinates utilizing a 40-point Gaussian quadrature. Details of this solution method can be found in texts on radiation such as Brewster.[11] Several cases were tested using a 48-point quadrature, and the difference in results between the 40 and 48 points was insignificant. Note that the high-order Gaussian quadrature is generally required in the calculation for real materials to accurately account for the fine angular structure of the scattering phase function. The solution yields the angular distributions of the transmitted and reflected intensities, from which the hemispherical reflectance is calculated as

$$R_{h\lambda} = \pi \int_{-1}^{0} I_\lambda(\mu, y = 0)\mu \frac{d\mu}{I_o} \tag{10}$$

The normal transmittance is calculated by

$$T_{n\lambda} = \pi \int_{\Delta\Omega} I_\lambda(\mu, y = L) \frac{d\Omega}{I_o} \tag{11}$$

where $\Delta\Omega$ is the solid angle subtended by the detector.

Experiment

Apparatus

Spectral reflectance and transmittance measurements for near normal incidence were made at room temperature using two reflectometers. For the visible to near infrared wavelength region (0.26–2.50 μm), a Gier–Dunkle model SP-250 spectrophotometer with an integrating sphere attachment was used. From 1.5 to 6.5 μm, measurements were made by utilizing a Gier–Dunkle model HC-300 heated cavity reflectometer.

The model SP-250 reflectometer consists of xenon arc and tungsten strip filament lamps for energy sources, monochromator with fused silica prism, transfer optics for specimen illumination, and a 20-cm-diam magnesium oxide-coated integrating sphere for the collection of reflected or transmitted energy. The test specimen is a nominally 2.7-cm diam disk that is positioned in the center of the sphere for reflectance measurements or over the 2.54-cm diam entrance port of the sphere for transmittance measurements. The central region of the sample is illuminated by a focused beam of monochromatic energy having a convergence angle of approximately 3 deg, and the size of the illuminated area on the sample is 0.3 by 0.6 cm. Measurement of spectral hemispherical reflectance for near-normal incidence is made with the sample rotated for an incidence angle of 15 deg from the normal to the plane of the sample surface. Transmittance measurements are made with the incident beam normal to the sample surface. At each wavelength the monochromatic beam is first directed onto the sphere wall to give the value of the incident intensity I_o. The beam is then directed onto the surface of the specimen to give the hemispherically collected reflected or transmitted intensity I. The value of the spectral transmittance or reflectance is I/I_o. The maximum uncertainties for the reflectance and transmittance measurements are 0.005 reflectance units and 0.001 transmittance units.

Measurements over the wavelength interval of 1.5–7.0 μm for directional spectral reflectance for hemispherical illumination and for normal spectral transmittance for normal incidence are made using a Gier–Dunkle model HC-300 reflectometer.[12] In the reflectance mode, the specimen is mounted on a water-cooled substrate having a diffuse reflectance of 0.04 or less over the wavelength interval of 1.5–6.5 μm. Energy reflected from the specimen at a 7-deg angle with respect to a normal to the specimen surface is collected in a 0.024-sr solid angle. By reciprocity, the reflectance of a material irradiated at a given angle of incidence as measured by the energy collected over the total hemisphere of reflection is equal to the reflectance for uniform irradiation from the hemisphere as measured by the energy collected at a single angle of reflection. Spectral normal transmittance is measured by placing the sample over the entrance slit of the monochromator section of the reflectometer. Energy from the heated cavity is directed onto the specimen with an illuminated area 2 cm in diameter. The maximum uncertainty in reflectance is 0.005 reflectance units, and the maximum uncertainty in transmittance is 0.0002.

Test Specimens

Fiber-loaded aerogels with various prescribed fiber mass fractions were fabricated in the form of rectangular bars with dimensions nominally 2.5 by 5 by 15 cm. Unloaded silica aerogels were also fabricated for reference measurements of the aerogel density and spectral absorption coefficient. Test specimens were machined from the bar to the desired thicknesses. Sample thicknesses for reflectance measurements were varied from 0.1 to 2.3 cm to cover a range of optical thicknesses between 5 and greater than 100. Thicknesses between 0.1–0.4 cm were used for spectral transmittance measurements. The maximum specimen thickness for transmittance measurements was determined based on the fiber volume fraction to keep the lower limit of transmittance greater than the minimum detectable value of 0.00005 for the test apparatus.

Scanning electron microscopy (SEM) was used to assess the fiber orientation and to determine the fiber size distribution. An SEM of a typical silica fiber specimen is shown in Fig. 1. The fibers appear to be randomly oriented in space and a large dispersion of fiber diameters is observed. Each individual specimen was carefully dimensioned and weighed. The solid volume fraction of each component in a specimen is computed as the product of the component mass fraction and the ratio of the density of the fibrous aerogel to that of the component material. The density of unloaded silica aerogel from dimensional and weight measurements is 0.124 gm/cm^3. The density of silica and alumina is 2.2 and 3.3 gm/cm^3, respectively. The

Fig. 1 SEM of silica fibers in silica aerogel.

Table 1 Summary of the compositions of the silica aerogel test specimens

Fiber type	Fiber wt%	Bulk density, gm/cm^3	Solid volume fraction	Fiber volume fraction
Silica	20	0.104	0.04545	0.00909
	25	0.124	0.05636	0.01409
	30	0.125	0.05682	0.01705
Alumina	15	0.148	0.06276	0.00558
	25	0.154	0.06217	0.00967
	35	0.169	0.06479	0.01486

total solid volume fraction is obtained by summing the component solid volume fractions. The estimated maximum uncertainties in fiber volume fraction and thickness are 6.5 and 4.5%, respectively. The compositions of the test specimens applied in the present study are summarized in Table 1.

Results

The assumption that unloaded silica aerogel is a purely absorbing medium is first verified by measuring its spectral normal transmittance. Transmittance measurements made 7 deg off-normal showed no detectable energy over the wavelength region from 1.0 to 3.0 μm, indicating that infrared scattering in the pure aerogel was insignificant compared with that from fibers. In the visible wavelength regime, there appeared to be a very small amount of scattering from the surfaces of the test specimens. The small amount of scattering will result in a calculated absorption coefficient slightly larger than the true value for wavelengths less than 1 μm. However, the interior regions of the aerogel appeared to the unaided eye to be clear without any haze.

An estimate was also made of the real part of the complex refractive index n of the unloaded silica aerogel, using the analysis of Caren[13] for the optical properties of a finely divided, high-porosity medium in the long wavelength limit. The value of n is estimated to lie between 1.004–1.042 over the range of wavelengths and aerogel densities of this study, indicating that Fresnel effects resulting from the aerogel matrix are negligible. These results support the assumption that unloaded aerogel can be treated as a purely absorbing medium. Figure 2 shows the aerogel spectral absorption coefficient determined from the Beer–Lambert law by utilizing the measured transmittance. The silica aerogel is very transparent to radiation in the wavelength regions of less than 0.5–2.5 μm and between 3.5–4.5 μm.

The present theoretical model requires only deterministic material properties for the calculation of the radiative properties of the fiber-loaded aerogels. These properties include the fiber size distribution, the solid volume fractions of the fibers and the fibrous aerogel, the spectral absorption coefficient of the unloaded aerogel, and the spectral refractive index of the fiber material, which are all a priori known physical parameters prescribed in the design of the material. The optical properties of the silica and alumina fibers are based on the data of Refs. 14 and 15. Prediction of the spectral transmittance and reflectance follows directly from the solution of the RTE utilizing these radiative properties and does not involve the empirical fitting of parameters that is inherent in an inversion approach. The silica fiber size distribution from SEM analysis of the raw fibers is shown in Fig. 3. The distribution is based on a sample population of 50 fibers. The mean diameter of the silica fibers is 2.38 μm. The mean diameter of the alumina fibers is 3.17 μm, as provided by the manufacturer.

Prediction of the spectral transmittance and reflectance as outlined in Eq. (8–11) requires the radiative coefficients and scattering phase function of the dispersed fibers at each wavelength based on Eqs. (5–7). This involves a significant amount of computation because these properties must be evaluated for each fiber diameter and then summed according to the size distribution at each wavelength. The numerical calculations were performed on a Pentium-100 personal computer system, which typically required about 1 h for the entire spectral region of interest. For the purpose of illustration, the predicted spectral extinction coefficients of the aerogels for specific loadings of silica and alumina fibers are shown in Fig. 4. The product of scattering coefficient and phase function $\langle \sigma_{s\lambda} p_\lambda(\eta) \rangle$, at two different wavelengths for the polydispersion of silica fibers and monosize alumina fibers, are shown in Fig. 5. Note that $\langle \sigma_{s\lambda} p_\lambda(\eta) \rangle$ is computed by utilizing Eqs. (6) and (7) according to the composition of each specimen at each wavelength.

The sensitivity of the predicted normal transmittance to the assumption of fiber size distribution is illustrated in Fig. 6 for a 0.24-cm-thick specimen containing 20 wt% of the silica fibers. Predictions based on the actual fiber size distribution (cf. Fig. 3) are compared with those based on the mean diameter of 2.38 μm. The agreement between theory and experiment is generally better when the actual size distribution is used. However, the accuracy of the prediction is not strongly compromised by using a mean fiber diameter (monosize calculation) when the fiber size distribution is a continuous function with

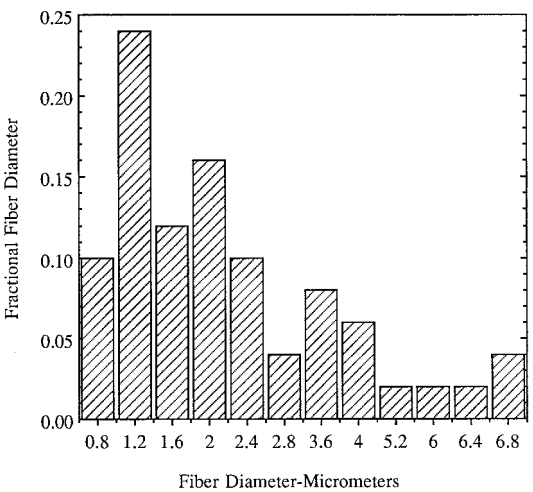

Fig. 3 Size distribution of silica fibers.

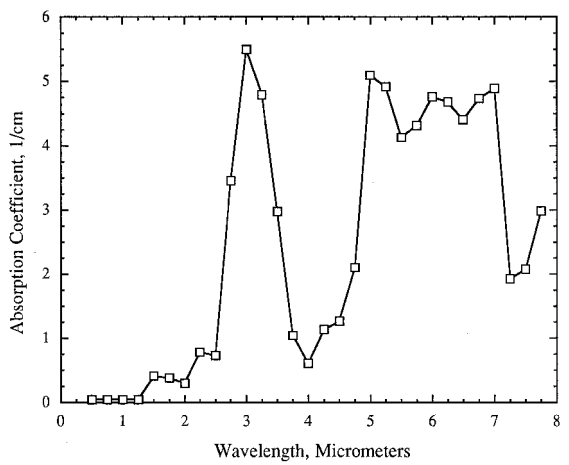

Fig. 2 Measured absorption coefficient of unloaded silica aerogel.

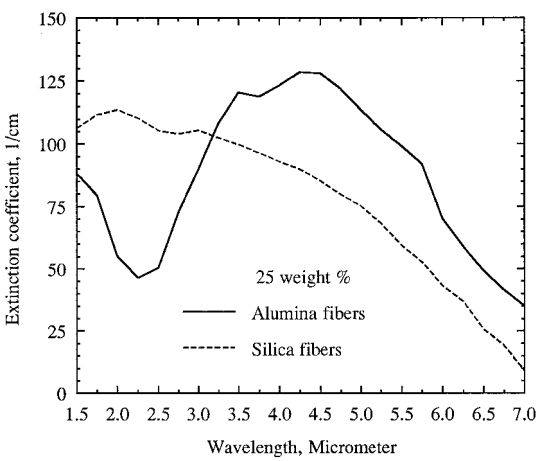

Fig. 4 Predicted extinction coefficients of randomly oriented silica and alumina fibers.

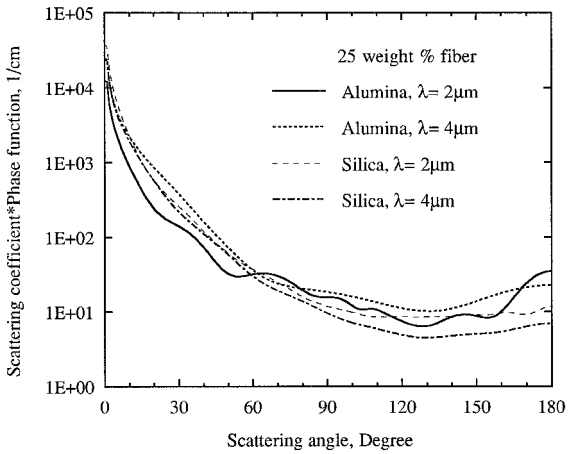

Fig. 5 Product of scattering coefficient and phase function at two different wavelengths for silica and alumina fibers.

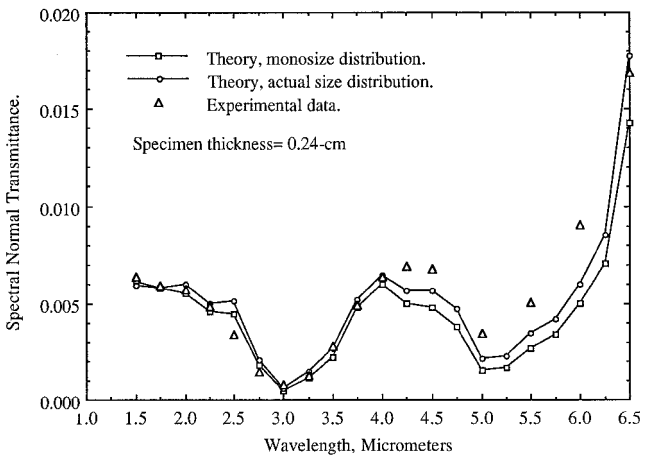

Fig. 6 Comparison of experiment and theory based on the actual fiber size distribution and the mean diameter for a fiber-loaded silica aerogel.

a small variance. The difference in the predicted spectral transmittance based on the monosize and the actual size distribution varies between 10–20%, depending upon wavelength, for this material. The agreement between theory using the actual size distribution and experiment is typically of the order of 5–10%. Similar comparisons and results were also obtained for specimens of different fiber loadings.

Figure 7 illustrates the typical agreement observed between theoretical predictions utilizing the actual size distribution and experimental data for normal spectral transmittance of silica aerogel loaded with 25 and 30 wt% silica fibers. Specimen thickness is 0.32 cm in each case. The agreement of the spectral variation in transmittance between theory and experiment is excellent. This demonstrates the validity of the modeling approach with regard to both fiber radiative properties and the treatment of the aerogel absorption as well as the spectrally-dependent optical properties of the fiber and matrix materials. Agreement between absolute values of transmittance is also generally quite good. However, the effects of local variations in fiber volume fraction and aerogel solid fraction have a strong influence on the absolute values. The differences between theory and experiment for transmittance values (e.g., in Fig. 7a for wavelengths between 5–6.5 μm) are believed to be the result of local variations in fiber and aerogel densities in the bulk material from which the individual specimens are taken. Figure 8 shows the comparison between theory and experiment for the spectral hemispherical reflectance of aerogels loaded with 25 wt% of silica fibers for two thicknesses. Again, the agreement between theory and experiment is very good.

Comparisons between the theory and experiment for silica aerogels loaded with different weight percent of alumina fibers are given in Figs. 9 and 10. Both the fiber diameter and fiber composition data were supplied by the vendor. Fiber composition was given as 96–97% Al_2O_3, with the balance SiO_2. The theoretical predictions were made using a monosize fiber diameter of 3.17 μm and the complex refractive index of sapphire.[15] Figure 9 shows the comparison for 25 wt% alumina fibers for specimen thicknesses of 0.64 and 1.02 cm. The comparison for 15 and 35 wt% alumina fibers for a specimen thickness of 2.3 cm is shown in Fig. 10. The agreement is very

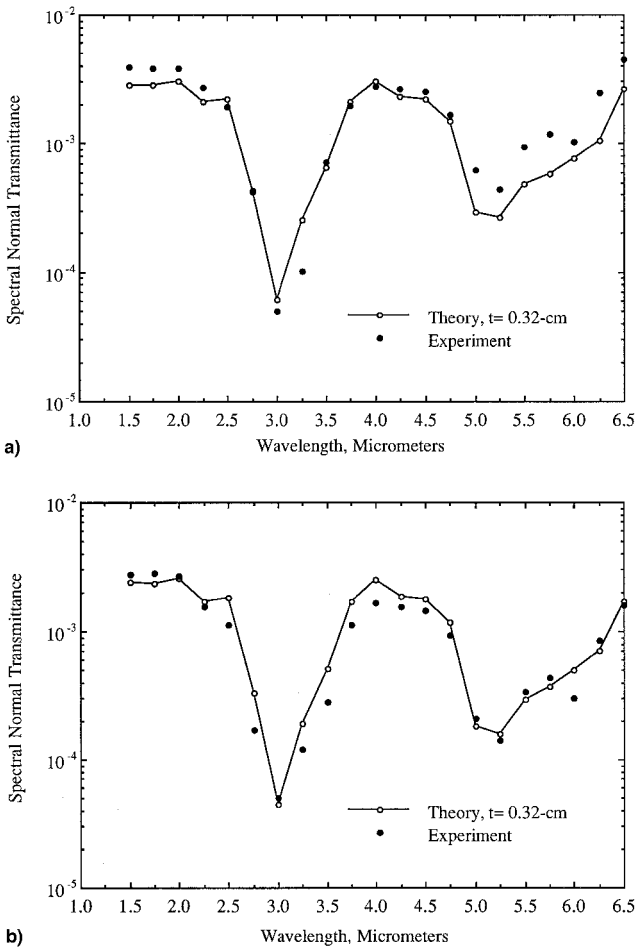

Fig. 7 Comparison of experiment and theory for fiber-loaded silica aerogel: a) 25 and b) 30 wt% silica fiber.

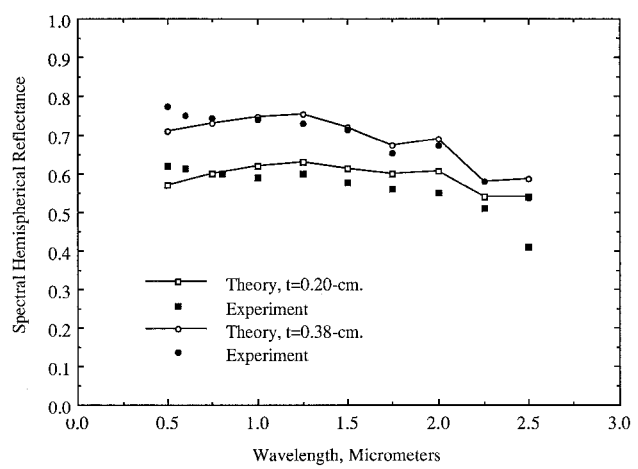

Fig. 8 Comparison of the theoretical and measured hemispherical reflectance for 25 wt% silica fiber loaded silica aerogel.

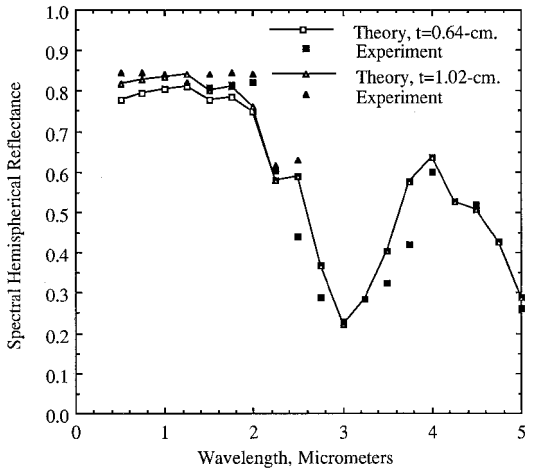

Fig. 9 Comparison of the theoretical and measured hemispherical reflectance for 25 wt% alumina fibers in silica aerogel.

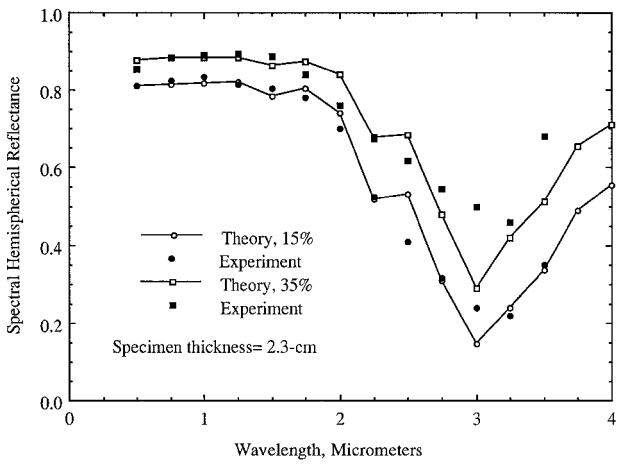

Fig. 10 Comparison of theoretical and measured hemispherical reflectances for 15 and 35 wt% alumina fibers in silica aerogel.

good in all cases. The strong decrease in reflectance in the 2.5–3.5 μm spectral region is because of the strong absorption of the aerogel matrix. Reflectance increases at 4 μm where the aerogel is weakly absorbing and scattering by the alumina fibers governs the radiative properties of the composite. Reflectance then again decreases with increasing wavelength as the aerogel absorption becomes stronger.

Conclusions

The validity of a theoretical model for the radiative properties of high-porosity, fiber-loaded aerogels is demonstrated by the excellent agreement between the predicted and measured spectral reflectance and transmittance of these composites over the visible and infrared wavelengths. Specimens used in the experiment include silica aerogels of various thicknesses loaded with different mass fractions of alumina and silica fibers. The theoretical model consists of treating the extinction coefficient of the fiber-loaded aerogel composites as the sum of the extinction coefficients of the fibers and that of the purely absorbing aerogel. The spectral radiative coefficients and scattering phase function of fibers are formulated from fundamental theory.

The fiber radiative properties and the spectral reflectance and transmittance are computed by utilizing deterministic properties of the material composition. Agreement between the theoretical predictions and experiment is not guaranteed, because there is no empirically adjusted parameter in the present theory. This rigorous theoretical approach contrasts with the empirical fitting analyses, commonly known as the inversion method, which enforce the agreement by a somewhat arbitrary adjustment of unknown constants in the model. Typical inversion analyses were summarized in Ref. 6. The radiative properties obtained from the inversion analyses are, of course, only applicable to the specimens whose data are utilized in the inversion.

Because the present theory does not involve any empirical adjustment, the good agreement between prediction and experiment demonstrates the validity of the theoretical formulations. The present model can accurately predict the influence of material composition on the radiative properties of composites of fibers in an absorbing matrix such as aerogel, and thereby be used to optimize the thermal performance. The present study also indicated that if the fibers exhibit a continuous, rather than multimodal, size distribution, a mean fiber diameter can be used in place of the actual size distribution when accuracies of the order of 20% are acceptable. The monosize assumption can greatly reduce the computational time.

Acknowledgment

This work was supported by NASA Ames Research Center under Contract NAS2-13897.

References

[1]Kistler, S. S., "Coherent Expanded Aerogels and Jellies," *Nature*, Vol. 127, 1931, p. 741.

[2]Caps, R., and Fricke, J., "Infrared Radiation Heat Transfer in Highly Transparent Silica Aerogel," *Solar Energy*, Vol. 36, 1986, pp. 361–365.

[3]Fricke, J., Lu, X., Wang, P., Buttner, D., and Heinemann, U., "Optimization of Monolithic Silica Aerogel Insulants," *International Journal of Heat and Mass Transfer*, Vol. 35, No. 9, 1992, pp. 2305–2309.

[4]Schwertfeger, F., Kuhn, J., Bock, V., Arduini-Schuster, M. C., Seyfried, E., Schubert, U., and Fricke, J., "Infrared Opacification of Organically Modified SiO_2 Aerogels via Pyrolysis," *Proceedings of the 22nd Thermal Conductivity Conference*, Technomic, Lancaster, PA, 1993, pp. 589–598.

[5]Hrubesh, L. W., and Pekala, R. W., "Thermal Properties of Organic and Inorganic Aerogels," Lawrence Livermore National Lab., UCRL-JC-111333, Livermore, CA, 1993.

[6]Cunnington, G. R., and Lee, S. C., "Radiative Properties of Fibrous Insulations: Theory Versus Experiment," *Journal of Thermophysics and Heat Transfer*, Vol. 10, No. 3, 1996, pp. 460–466.

[7]Kerker, M., *The Scattering of Light and Other Electromagnetic Radiation*, Academic, New York, 1969, Chap. 6.

[8]Lee, S. C., "Radiative Transfer Through a Fibrous Medium: Allowance for Fiber Orientation," *Journal of Quantitative Spectroscopy and Radiative Transfer*, Vol. 36, No. 3, 1986, pp. 253–263.

[9]Lee, S. C., "Effect of Fiber Orientation on Thermal Radiation in Fibrous Media," *International Journal of Heat and Mass Transfer*, Vol. 32, No. 2, 1989, pp. 311–319.

[10]Lee, S. C., "Scattering Phase Function for Fibrous Media," *International Journal of Heat and Mass Transfer*, Vol. 33, No. 10, 1990, pp. 2183–2190.

[11]Brewster, M. Q., *Thermal Radiative Transfer and Properties*, Wiley, New York, 1992, Chap. 12.

[12]Dunkle, R. V., Edwards, D. K., Gier, J. T., Nelson, K. E., and Roddick, R. D., "Heated Cavity Reflectometer for Angular Reflectance Measurements," *Progress in International Research on Thermodynamic and Transport Properties*, Academic Press, New York, 1962.

[13]Caren, R. P., "Radiation Transfer from a Metal to a Finely Divided Particulate Medium," *Journal of Heat Transfer*, Vol. 93, Feb. 1969, pp. 154–156.

[14]Palik, E. D. (ed.), *Handbook of Optical Constants of Solids II*, Academic, New York, 1991.

[15]Malitson, I. H., Murphy, F. V., and Rodney, W. S., "Refractive Index of Synthetic Sapphire," *Journal of Optical Society of America*, Vol. 48, 1958, p. 72.